Am J Cancer Res 2023;13(5):1766-1785
www.ajcr.us /ISSN:2156-6976/ajcr0148908

Original Article

NPM1 promotes nasopharyngeal carcinoma metastasis and stemness by recruiting Mdm2 to induce the ubiquitination-mediated degradation of p53

Liya Hu[1,2*], Pinggui Gong[1,2*], Ni Zhou[1], Shuilian Wang[1], Cui He[2], Yixuan Zhou[1,2], Qiwen Li[2,3], Xueman Zhao[2,4], Hong Peng[1,2]

[1]The Second School of Clinical Medicine, Southern Medical University, Guangzhou 510515, Guangdong, China; [2]Department of Otolaryngology-Head and Neck Surgery, Guangdong Second Provincial General Hospital, Guangzhou 510220, Guangdong, China; [3]Hengyang Medical College, University of South China, Hengyang 421001, Hunan, China; [4]School of Medicine, Jinan University, Guangzhou 510632, Guangdong, China. [*]Equal contributors.

Received January 3, 2023; Accepted April 13, 2023; Epub May 15, 2023; Published May 30, 2023

Abstract: Nasopharyngeal carcinoma (NPC) is clinically challenging due to the development of distant metastasis following initial therapy. Therefore, it is necessary to elucidate the mechanisms underlying metastases to develop novel therapeutic strategies. Nucleophosmin 1 (NPM1) has been directly linked to the development of human tumors and may have both tumor-suppressing and oncogenic properties. Although NPM1 is often overexpressed in solid tumors of various histopathological origins, its specific function in mediating the development of NPC is still unknown. Here, we investigated the role of NPM1 in NPC and discovered that NPM1 was elevated in clinical NPC samples and served as a predictor of the worst prognosis in NPC patients. Furthermore, the upregulation of NPM1 promoted the migration and the cancer stemness of NPC both in vitro and in vivo. Mechanistic analyses revealed that the E3 ubiquitin ligase Mdm2 was recruited by NPM1 to induce the ubiquitination-mediated proteasomal degradation of p53. Ultimately, knockdown of NPM1 suppressed the stemness and EMT signals. In summation, this study demonstrated the role and the underlying molecular mechanism of NPM1 in NPC, providing the evidence for the clinical application of NPM1 as a therapeutic target for the treatment of patients with NPC.

Keywords: Nasopharyngeal carcinoma, NPM1, metastasis, cancer stemness, p53, ubiquitin degradation, EMT

Introduction

Nasopharyngeal carcinoma (NPC), which is originated from the nasopharynx mucosal lining and is highly prevalent in South China [1], has a strong tendency for local invasion as well as early distant metastases in the nasopharynx [2, 3]. It is suggested that patients with the early stages of NPC should receive radiotherapy, while those with the late stages are best treated with chemoradiotherapy [4]. In recent years, the 5-year survival period of NPC patients has been significantly improved, but recurrence and metastasis are still the most common causes of mortality in NPC patients [5]. Therefore, understanding the biological and molecular processes underpinning NPC metastasis would assist in developing effective treatment approaches for this particular type of cancer.

Nucleophosmin (NPM), also known as B23, numatrin, and NO38, is a nucleolar phosphoprotein that continuously shuttles between the cytoplasm and nucleus [6]. NPM exists in two alternatively spliced isoforms of NPM1 and NPM2 (B23.1 and B23.2, respectively), with NPM1 being the predominant type in all tissues [7, 8]. NPM1 contains distinct functional domains that perform unique biochemical functions [9].

It has been reported that NPM1 is engaged in cellular processes that are closely linked to both growth-inhibiting and proliferation-promoting pathways. NPM1 is also involved in apopto-

sis in response to stress and carcinogenic irritations, such as DNA damage and hypoxia. Furthermore, NPM1 has been shown to directly link to tumor development, as its expression is upregulated in a variety of tumors; hence, NPM1 is regarded as a diagnostic marker for gastric [10], colon [11], ovarian [12], and prostate carcinomas [13]. In line with this, the expression of NPM1 is also correlated with the stage of tumor progression. For example, the overexpression of NPM1 mRNA is independently associated with the recurrence of bladder carcinoma as well as its progression to a more advanced stage [14]. However, little research has been conducted to explore the role of NPM1 in NPC.

Epithelial-mesenchymal transition (EMT) and cancer stem cells (CSCs) are two important factors contributing to cancer metastasis. Regarding the first of these factors, epithelial cells undergo a unique process called EMT, during which, they acquire mesenchymal stem cell qualities [15]. EMT can also be conducive to tumor cell progression, drug resistance, and metastasis [16]. Regarding the second of these factors, a subpopulation of tumor cells that possess the capacities of limitless self-renewal and differentiation are collectively known as cancer stem cells (CSCs), which are also referred to as tumor-initiating cells [17, 18]. More importantly, CSCs exhibit enhanced resistance to chemotherapy and radiotherapy, and hence are frequently responsible for the poor treatment response, recurrence, and metastasis [19].

Previous studies have shown that NPM1 can regulate the stability and function of essential tumor-suppressor proteins [20], among which, p53, is known for its critical role in cell cycle arrest, cellular senescence, and apoptosis. Posttranslational modifications, including acetylation, ubiquitination, and phosphorylation, primarily modulate the abundance and activity of p53 [21-23]. Numerous investigations have revealed ubiquitination to be the most important posttranslational modification process of p53 [24, 25]. Notably, oncoprotein Mdm2 is a potent inhibitor of p53 [26], and Mdm2 is frequently overexpressed in different types of cancer and is negatively correlated with p53 levels, leading to low survival and poor prognosis.

In this study, we demonstrate for the first time that NPM1 is elevated in NPC relative to normal tissues, and is associated with the poor prognosis of NPC patients. Mechanistically, NPM1 interacts with p53 and enhances the pathway for the ubiquitin-mediated proteasomal degradation of p53, which in turn promotes NPC metastasis and stemness. As a result, NPM1 could be a potential therapeutic target for the treatment of NPC.

Material and methods

Clinical specimens

All tissue specimens used in this study were collected from Guangdong Second Provincial General Hospital. This study was approved by the Ethics Committee of Guangdong Second Provincial General Hospital, and written informed consent was obtained from all patients.

Cell culture

Human NPC cell lines (5-8F, HONE1, SUNE1, HONE1-EBV+, and 6-10B) and a human immortalized nasopharyngeal epithelium cell line (NP69) were acquired from the Central Laboratory of the Integrated Hospital of Traditional Chinese Medicine of the Southern Medical University. The NPC cells were cultured in RPMI-1640 (Gibco, Carlsbad, CA, USA) with 10% fetal bovine serum (FBS, Gibco, Carlsbad, CA, USA), while the NP69 cells were grown in a keratinocyte serum-free medium (Gibco, Grand Island, NY, USA) supplemented with prequalified human recombinant epidermal growth factor. All cells were maintained at 37°C in a humidified atmosphere of 5% CO_2.

Lentivirus production and infection

The Human *NPM1* gene was inserted into the GV344 lentiviral vector to generate NPM1-expressing lentivirus (LV-NPM1) (GeneChem, Shanghai, China). Lentivirus containing an empty GV344 vector (LV-NC) was used as the negative control (GeneChem, Shanghai, China). 5-8F and HONE1 cells were infected with either the NPM1-expressing or control vector lentivirus. Polyclonal cells expressing the luciferase marker protein were selected for further experiments.

Transient transfection

Small interfering RNAs (siRNAs) targeting *p53* or *Mdm2* were purchased from Ribobio (Guangzhou, China). The siRNA sequences were as follows: sip53-2: ACACGACATTGGCATAATT; siMdm2-3: GTAACCCAATGATGTATGA. Plasmids for NPM1 overexpression were constructed by GeneChem (Shanghai, China). Lipofectamine 3000 (Invitrogen, Waltham, MA, USA) was used to transfect the plasmids and siRNA according to the manufacturer's instruction.

RNA extraction and quantitative real-time polymerase chain reaction (qPCR)

Total RNA was extracted from cells using the Cell Total RNA Isolation Kit (Foregene, China). After measuring the RNA concentration, cDNA was synthesized using a reverse transcription kit (TaKaRa, Dalian, China). qPCR was carried out using SYBR Premix Ex Taq (TaKaRa, Dalian, China). The primer sequences were as follows: NPM1 forward: ACGGTCAGTTTAGGGGCTG, NPM1 reverse: CTGTGGAACCTTGCTACCACC, p53 forward: CAGCACATGACGGAGGTTGT, p53 reverse: TCATCCAAATACTCCACACGC, GAPDH forward: GCACCGTCAAGGCTGAGAAC, GAPDH reverse: TGGTGAAGACGCCAGTGGA.

Western blot analysis

Total protein was extracted from cells using RIPA lysis buffer combined with a mixture of protease and phosphorylase inhibitors, quantified using BCA protein assay kit (Thermo Scientific, Waltham, MA, USA). After quantification, sodium dodecyl sulfate-polyacrylamide gel electrophoresis (SDS-PAGE) was performed to separate 30 μg of the total protein. Then, the separated proteins were transferred onto polyvinylidene fluoride (PVDF) membranes for further immunoblotting with specific antibodies. The primary antibodies used were as follows: anti-E-cadherin (Proteintech, 1:1000), anti-N-cadherin (Proteintech, 1:1000), anti-NPM1 (Proteintech, 1:5000), anti-vimentin (Proteintech, 1:2000), anti-tubulin (Bioworlde, 1:5000), anti-Mdm2 (Proteintech, 1:1000), anti-p53 (Proteintech, 1:2000), anti-GAPDH (Bioworlde, 1:15000), anti-CD44 (CST, 1:1000), anti-SOX2 (Proteintech, 1:1000), anti-NANOG (Proteintech, 1:1000), anti-OCT4 (Proteintech, 1:1000), and anti-ubiquitin (Proteintech, 1:1000). After overnight incubation with the primary antibodies, the membranes were incubated with HRP-conjugated secondary antibodies at room temperature for 1 h. An enhanced chemiluminescence reagent kit (Thermo Scientific, Waltham, MA, USA) was then utilized to detect the target proteins. Images were photographed using a Bio-Rad ChemiDoc XRS+ Imager.

Immunohistochemistry (IHC) staining

Tissue samples from the nasopharynx of forty patients (including 20 NPC samples and 20 noncancerous nasopharyngeal samples) were collected from Guangdong Second Provincial General Hospital of Southern Medical University. These tissue samples were fixed, embedded with paraffin, and then cut into sections. In addition, NPC tissue microarrays (HNasN110Su01) were purchased from Outdo Biotech (Shanghai, China). The tissue sections and the tissue microarrays were examined by IHC staining. Briefly, the samples underwent xylene deparaffinization and ethanol gradient rehydration. Subsequently, the samples were exposed to sodium citrate for antigen retrieval and goat serum was used to block any non-specific binding sites. Then, the samples were stained with primary antibodies and incubated at 4°C overnight. The antibody used in IHC were anti-NPM1 (Proteintech, 1:200), anti-E-cadherin (Proteintech, 1:250), anti-N-cadherin (Proteintech, 1:250), anti-CD44 (CST, 1:100), anti-CD133 (Proteintech, 1:100), anti-OCT4 (Proteintech, 1:250). After extensive washing, the samples were incubated in the corresponding goat anti-rabbit IgG and streptavidin peroxidase (SP) complex at 37°C for 30 min, followed by staining with DAB solution. Finally, the samples were stained with hematoxylin, air dried, and imaged under a microscope.

Wound healing assay

Cells were seeded in six-well plates and cultured overnight. When the cell confluence reached approximately 90%, a 10 μl pipette tip was used for wound scratching. The cells were then cultured in serum free RPMI 1640 medium for indicated time. Cell images to taken to compare the reduction of the wound area due to cell migration. ImageJ software was used to measure the optical scratch wound regions.

Transwell assay

Cell migration was assessed using transwell filter chambers (Corning, NY, USA) in 24-well plates without Matrigel (BD Biosciences). Briefly, 1×10^5 cells in serum-free medium were seeded in the upper chamber while complete medium with 10% FBS was added to the lower chamber. After 15 h of incubation, the top side of the upper chambers was gently swabbed with cotton-tipped applicators and the underside cells from migration were fixed with paraformaldehyde for 30 minutes, followed by 0.1% crystal violet staining for 20 minutes. Finally, the migrated cells were counted in three randomly chosen fields under inverted microscope.

Tumorsphere formation assay

NPC cells (5×10^3) were trypsinized, suspended, counted, and seeded into ultra-low attachment 6-well plates (Coring, USA). Then, NPC cells were propagated in a final volume of 2 ml of serum-free DMEM/F12 medium containing 2% B27 (Invitrogen Biotechnology, China), 20 ng/ml epidermal growth factor (Invitrogen Biotechnology, China), and 20 ng/ml fibroblast growth factor (Invitrogen Biotechnology, China) for 14 days. Fresh medium was added against the sides of the well every 3 days, and spheroids in three randomly selected fields were counted.

Flow cytometry analysis

Single-cell suspension of NPC cells (1×10^6) in RPMI-1640 replenished with 2% fetal bovine serum was used for side population analyses. Briefly, Hoechst 33342 (5 μg/ml) (Sigma-Aldrich, MO, USA) was added to cautiously resuspend the cells every 10 min at 37°C for 90 min. In the negative control group, verapamil (50 μmol/l) (Sigma-Aldrich, MO, USA) was simultaneously administered to the samples. After washing with cold PBS, the cells were examined via flow cytometry. Dead cells were identified using propidium iodide staining.

Immunofluorescence staining and confocal microscopy

Cells (6×10^4) were trypsinized, suspended, counted, and seeded into a fluorescence culture dish and cultured overnight until cell adherence. The cells were then washed with PBS and fixed with 4% paraformaldehyde at room temperature for 1 h followed by permeabilization using 0.5% Triton X-100 for 15 minutes. Subsequently, the cells were stained with the indicated primary antibodies (CD44 (1:100), SOX2 (1:100), p53 (1:50), Mdm2 (1:100), and NPM1 (1:200)). The nuclei were stained by DAPI before the cells were examined with a fluorescent confocal microscope (Carl Zeiss LSM800, Germany).

Co-immunoprecipitation (Co-IP) assay

Co-IP assay was performed using a Pierce Coimmunoprecipitation Kit (Thermo Scientific, Waltham, MA, USA) to detect NPM1-interacting proteins. According to the manufacturer's instructions, proteins obtained from the 5-8F and HONE1 cells were collected and quantified. Then, 5 mg of the obtained protein was combined with either anti-specific-protein antibodies or control IgG before being incubated at 4°C overnight. Proteins that were co-precipitated with NPM1 were eluted and subjected to Mass spectrometry and western blot analyses.

Cycloheximide (CHX) chase assay

Prior to the experiment, CHX (Abcam, Massachusetts, USA) was suspended in DMSO (200 mM) and stored at -20°C. Cells with and without NPM1-overexpression were treated with 50 μg/ml CHX, harvested at different time points: 0, 20, 40, 60, 80, and 100 minutes, and extracted the relevant proteins. Subsequently, the obtained proteins were quantified and further analyzed by western blot analysis.

Ubiquitination assay

5-8F and HONE1 cells were transiently transfected with NPM1-overexpressing plasmids for at least 48 h and then treated with 20 μmol/L MG132 (Sigma-Aldrich, MO, USA) for 6 h. The cells were then lysed with IP lysis buffer to extract the total cell proteins. Protein A/G immunoprecipitation magnetic beads were treated with the cell lysates for 30 minutes at room temperature, and then they were subjected to Co-IP with the indicated antibodies or IgG. The magnetic beads were washed five times with washing buffer solution. After extensive washing, the proteins were then balanced with

protein sample buffer and released by boiling. Western blot analysis was performed.

Animal experiments

All experiments using animals were approved by and handled according to the guidelines of the Southern Medical University Animal Ethics Committee. To assess the effect of NPM1 on tumor growth in vivo, a mouse subcutaneous xenograft model was used. Female BALB/c nude mice (4 weeks old, 8-10 g) were purchased from SPF (Beijing) Biotechnology Co., Ltd (Beijing, China). Twenty mice were randomly assigned into four experimental groups (N = 5/group), and mice in each were subcutaneously injected with different number of 5-8F cells: 2×10^6, 1×10^6, 5×10^5, and 2×10^5/100 μl PBS, respectively. The 5-8F cells used for injection were control or NPM1 knockdown cells. They were injected in the left or right flank of mice, respectively. Tumor growth was monitored, and the mice were euthanized 15 days after cell inoculation. Tumor nodules were dissected, weighed, dried, paraffin-embedded and fixed for further analysis.

To study the effect of NPM1 on pulmonary metastasis, tail vein injection of tumor cells was performed. A total of 12 female 3-week-old BALB/c nude mice were randomly divided into two groups (N = 6/group) and received either control or NPM1 knockdown 5-8F cells, 2×10^6/100 μl injection via tail vein. Six weeks after injection, the lung tissue from each mouse was dissected, and the number of pulmonary metastatic nodules was counted and confirmed by H&E staining.

Statistical analysis

Statistical analysis was performed using IBM SPSS Statistics 26.0 (IBM, Armonk, NYC, USA). The data were presented as the mean ± SD of at least three independent repeated experiments. Comparisons between two groups were performed using Student's t-test, while comparisons among multiple groups were performed using one-way ANOVA. Kaplan-Meier analysis and the logarithmic rank test were utilized for survival analysis. The independent prognostic variables were examined using the Cox proportional hazard regression model. A *P*-value of < 0.05 indicated statistical significance.

Results

NPM1 was upregulated in NPC and associated with poor prognosis

To explore the role of NPM1 on NPC tumorigenesis, we first conducted a thorough exploration of the expression of NPM1 at the tissue and cellular levels. RNA-seq data obtained from the TCGA database revealed that NPM1 mRNA levels were increased in head and neck squamous cell carcinoma compared to normal tissues, as well as other tissues such as colon, liver, and lung (**Figure 1A**). Next, we investigated the impact of NPM1 on the prognosis of NPC patients by comparing NPM1 mRNA levels between noncancerous nasopharyngeal (NP) and NPC tissues using the data from GEO (Gene Expression Omnibus) databases (**Figure 1B**). We found that NPC patients with high levels of NPM1 expression had shorter overall survival (OS) and disease-free survival (DFS) than those with low levels of NPM1 expression (**Figure 1C**). Furthermore, NPM1 protein level was higher in several NPC cell lines than in the immortalized nasopharyngeal epithelial NP69 cells, as determined by Western blot analysis (**Figure 1D**). Moreover, we performed an immunohistochemistry analysis using 20 noncancerous nasopharyngeal tissues and 20 NPC tissues. NPM1 expression level was found to be substantially higher in NPC tissues than in noncancerous nasopharyngeal tissues, according to the immunohistochemical analysis (**Figure 1E**, **1F**). Notably, there was a significant correlation between NPM1 expression and several clinical characteristics, including age, TNM grade, histological grade and clinical stage. Kaplan-Meier analysis indicated that higher NPM1 levels were associated with poor OS and DFS of NPC patients. Consistently, NPM1 was positively correlated with AJCC stage, tumor size, prognosis, and tumor recurrence (**Table 1**). Univariate and multivariate regression analysis also suggested that NPM1 might be an important indicator for the OS and DFS of NPC patients (**Figure 1G**; **Table 2**). Together, these findings show that NPM1 was upregulated in NPC and was related to the clinicopathological features of NPC patients.

NPM1 promoted NPC cell migration and tumor stemness in vitro

Since we found an upregulation of NPM1 in NPC, we hypothesized that NPM1 might be

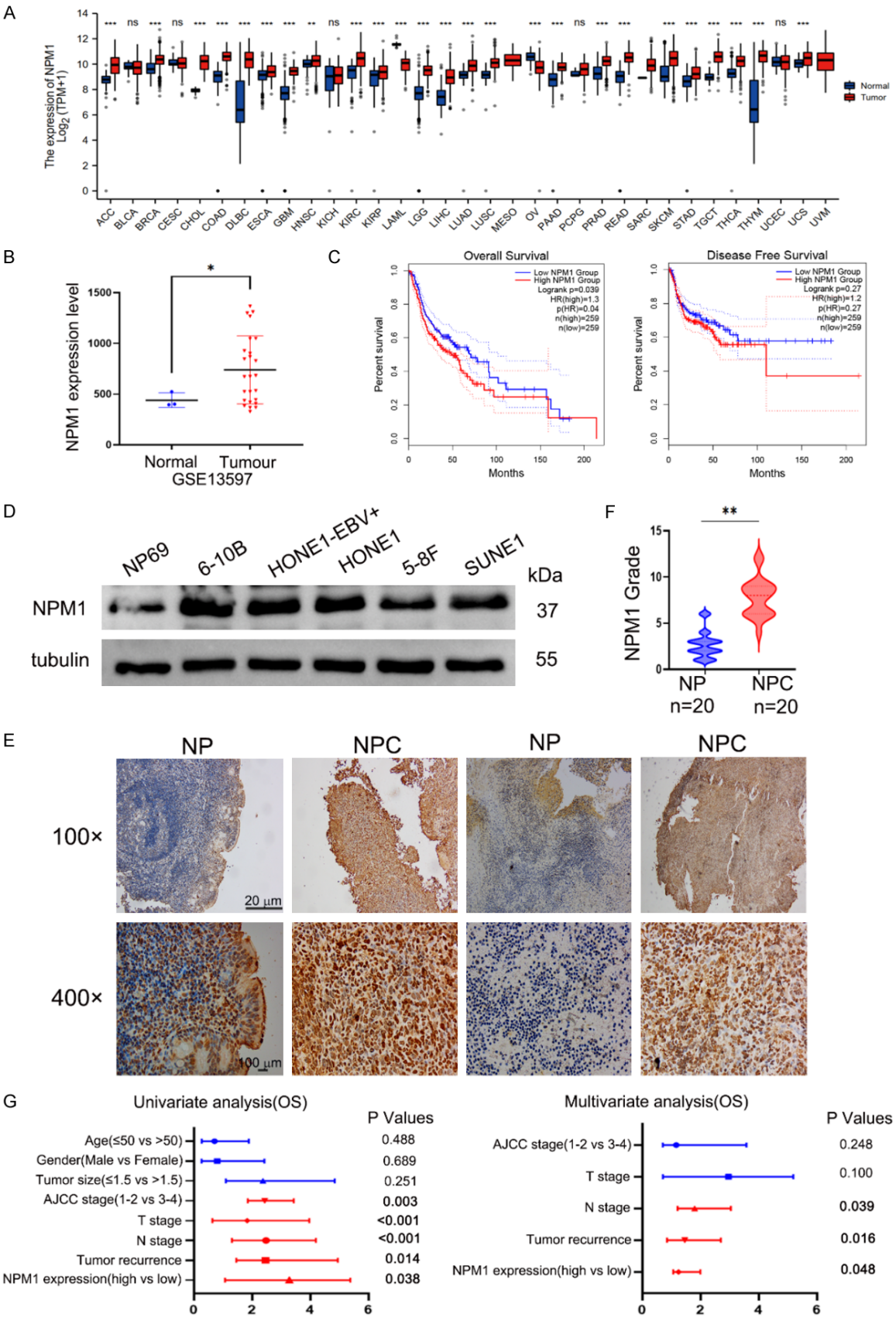
A
The expression of NPM1 Log2 (TPM+1)
Normal
Tumor
ACC BLCA BRCA CESC CHOL COAD DLBC ESCA GBM HNSC KICH KIRC KIRP LAML LGG LIHC LUAD LUSC MESO OV PAAD PCPG PRAD READ SARC SKCM STAD TGCT THCA THYM UCEC UCS UVM
B
NPM1 expression level
Normal
Tumour
GSE13597
C
Overall Survival
Disease Free Survival
Low NPM1 Group
High NPM1 Group
Percent survival
Months
D
NP69
6-10B
HONE1-EBV+
HONE1
5-8F
SUNE1
kDa
NPM1
tubulin
37
55
F
NPM1 Grade
NP
n=20
NPC
n=20
E
NP
NPC
100×
400×
20 μm
100 μm
G
Univariate analysis(OS)
P Values
Age(≤50 vs >50) 0.488
Gender(Male vs Female) 0.689
Tumor size(≤1.5 vs >1.5) 0.251
AJCC stage(1-2 vs 3-4) 0.003
T stage <0.001
N stage <0.001
Tumor recurrence 0.014
NPM1 expression(high vs low) 0.038
Multivariate analysis(OS)
AJCC stage(1-2 vs 3-4) 0.248
T stage 0.100
N stage 0.039
Tumor recurrence 0.016
NPM1 expression(high vs low) 0.048

Figure 1. Expression of NPM1 in NPC tissues and cell lines. (A) The mRNA levels of NPM1 in different malignancies and normal tissue deposited in TCGA database. (B) The expression of NPM1 in NPC samples from Gene Expression Omnibus (GEO) database. *P < 0.05, as determined by the Student's t-test. (C) Low NPM1 expression was correlated with better OS and DFS of head and neck squamous cell carcinoma in TCGA database. (D) NPM1 protein levels in NP69, 6-10B, HONE1-EBV$^+$, HONE1, 5-8F, and SUNE1 cells as determined by Western blot analysis. (E, F) Representative IHC images (E) and IHC scores (F) of NPM1 expression in NPC. Bar = 100 μm. **P < 0.01, as determined by the Student's t-test. (G) Univariate and multivariate analyses of different clinicopathological features in NPC patients.

Table 1. The basic information of 110 patients with NPC

Clinicopathological features	Number	Low expression, N (%)	High expression, N (%)	*P* value
Age				
≤50	66	32	34	0.755
>50	44	20	24	
Gender				
Male	80	37	43	0.969
Female	30	14	16	
Tumor size				
≤1.5 cm	87	54	33	0.007**
>1.5 cm	23	7	16	
AJCC stage				
I/II	57	33	24	0.003**
III/IV	53	16	37	
T stage				
T1/T2	68	40	28	0.019*
T3/T4	42	15	27	
N stage				
N0/N1	75	43	32	0.024*
N2/N3	35	12	23	
M stage				
M0	109	58	51	0.473
M1	1	0	1	
Tumor recurrence				
No	60	36	24	0.037*
Yes	50	20	30	

*P < 0.05, **P < 0.01. *χ^2 test was applied to access the correlation between the clinicopathologic parameters and NPM1 expression. NPC: Nasopharyngeal carcinoma.

involved in the etiology and pathogenesis of NPC. To test this, we selected 5-8F and HONE1 cells to undergo both NPM1-knockdown and overexpression. We introduced lentivirus into 5-8F and HONE1 cells to downregulate NPM1 for the establishment of NPM1-knockdown cells. To establish NPM1-overexpression, plasmids overexpressing NPM1 were introduced into 5-8F and HONE1 cells separately. We then detected the corresponding proteins. The successful knockdown or overexpression of NPM1 was confirmed by Western blot analysis as shown in (**Figures 2A**, **2B** and **4C**). Results from the wound healing and transwell assays showed that NPM1 knockdown significantly reduced, while NPM1 overexpression enhanced the migration of 5-8F and HONE1 cells (**Figure 2C-I**). In contrast, the overexpression of NPM1 markedly enhanced the migration of 5-8F and HONE1 cells (**Figure 4A**, **4B**, **4G**, **4H**). Additionally, we found that EMT markers like N-cadherin and vimentin were downregulated during epithelial-mesenchymal transition (EMT), whereas E-cadherin was upregulated, by NPM1 knockdown, as determined by western blot analysis to identify signals representative of EMT (**Figure 2J**). Conversely, NPM1-overexpression exhibited the opposite effect (**Figure 4C**).

Table 2. Univariate and multivariate Cox regression analysis in 110 NPC patients

Clinical characters	Overall survival		
	HR	95% CI	*P* value
Univariate analysis			
Age	0.707	0.265-1.885	0.488
Gender	0.797	0.262-2.421	0.689
Tumor size	2.367	1.097-4.838	0.251
AJCC stage	2.430	1.850-3.430	0.003**
T stage	1.829	0.633-3.965	0.000***
N stage	2.478	1.307-4.191	0.000***
Tumor recurrence	2.460	1.459-4.941	0.014*
NPM1 expression	3.278	1.068-5.374	0.038*
Multivariate analysis			
AJCC stage	1.161	0.701-3.573	0.248
T stage	2.962	0.708-5.186	0.100
N stage	1.796	1.209-3.037	0.039*
Tumor recurrence	1.459	0.847-2.695	0.016*
NPM1 expression	1.245	1.061-1.990	0.048*

*P < 0.05, **P < 0.01, ***P <0.001. T, tumor size; N, lymph node; HR, hazard ratio; 95% CI, 95% confidence interval.

We also investigated the tumor stemness characteristics to determine the effect of NPM1 on NPC tumorigenesis. The main agents that encourage malignant tumor phenotypes, like metastasis, are cancer stem cells (CSCs). Immunofluorescence staining showed that NPM1-knockdown cells exhibited significantly lower levels of CD44 and SOX2 expression compared to control groups (**Figure 3A**). Furthermore, flow cytometry analysis revealed that NPM1-knockdown cells exhibited a down-regulation of the side population ratio (**Figure 3B**, **3G**; **Table 3**). Conversely, NPM1 overexpression resulted in the opposite effects to those listed above in NPC cells (**Figure 4D**, **4E**, Supplementary Figure 1D, 1E; **Table 4**). Importantly, in tumorsphere formation assay, which reflects the CSC property of cancer cells in vitro, we found that the size and number of tumorspheres were smaller and fewer in NPM1-knockdown 5-8F and HONE1 cells than in the control cells. Hence, results from the tumorsphere formation assay show that NPM1 stimulated tumorsphere growth (**Figure 3E**, **3F**). In line with this finding, NPM1 knockdown also reduced the expression of CSC markers, such as CD44, NANOG, OCT4, and SOX2, according to the western blot analysis (**Figure 3C**, **3D**), while NPM1 overexpression in NPC cells exhibited the opposite results (**Figure 4C**), suggesting that NPM1 regulates the malignancy of NPC. These findings imply that NPM1 is crucial for maintaining the biological characteristics of NPC cells.

NPM1 enhanced the tumor stemness and metastasis of NPC cells in vivo

To confirm our findings from in vitro studies, we generated a lung metastasis model and a subcutaneous xenograft tumor model using lentivirus-infected 5-8F cells in BALB/C nude mice to explore the biological function of NPM1 in vivo. The nude mice were first randomly assigned into the NPM1-knockdown group and the control group. Each group contained six BALB/C nude mice with the same age and similar weights. To verify whether NPM1 can accelerate metastasis in vivo, 2×10^6 NPM1-knockdown or control 5-8F cells were injected into the tail vein of nude mice. Our results showed that, compared to the mice in the control group, the mice in NPM1-knockdown group exhibited a less degree of pulmonary metastasis (smaller in tumor size and fewer in number) six weeks after injections (**Figure 5A**, **5B**). Consistently, the pulmonary metastatic tissues in NPM1-knockdown group exhibited higher expression of E-cadherin (E-ca) and reduced expression of N-cadherin (N-ca) (**Figure 5C**). Hence, we found that NPM1 dramatically promoted NPC malignancy both in vitro and in vivo.

To evaluate the effect of NPM1 on regulating the CSC properties of NPC in vivo, we carried out limiting dilution assay. Twenty BALB/C nude mice were randomly divided into four groups (N = 5/group). Control and NPM1-knockdown 5-8F cells were respectively transplanted to the left and right flanks of the mice to generate xenograft tumors (Supplementary Figure 1A). Our results showed that the injection of 2×10^6, 1×10^6, 5×10^5, and 2×10^5 NPM1-knockdown 5-8F cells produced tumors at the rates of 80% (4/5), 40% (2/5), 20% (1/5) and 0% (0/5), respectively, while the injections of control cells produced tumors at the rates of 100% (5/5), 80% (4/5), 60% (3/5) and 20% (1/5), respectively (**Figure 5D**, **5E**). These results show that, compared to the control group, the xenograft weights were reduced and tumor development was suppressed in the NPM1-knockdown group (Supplementary Figure 1B). Consistently, IHC

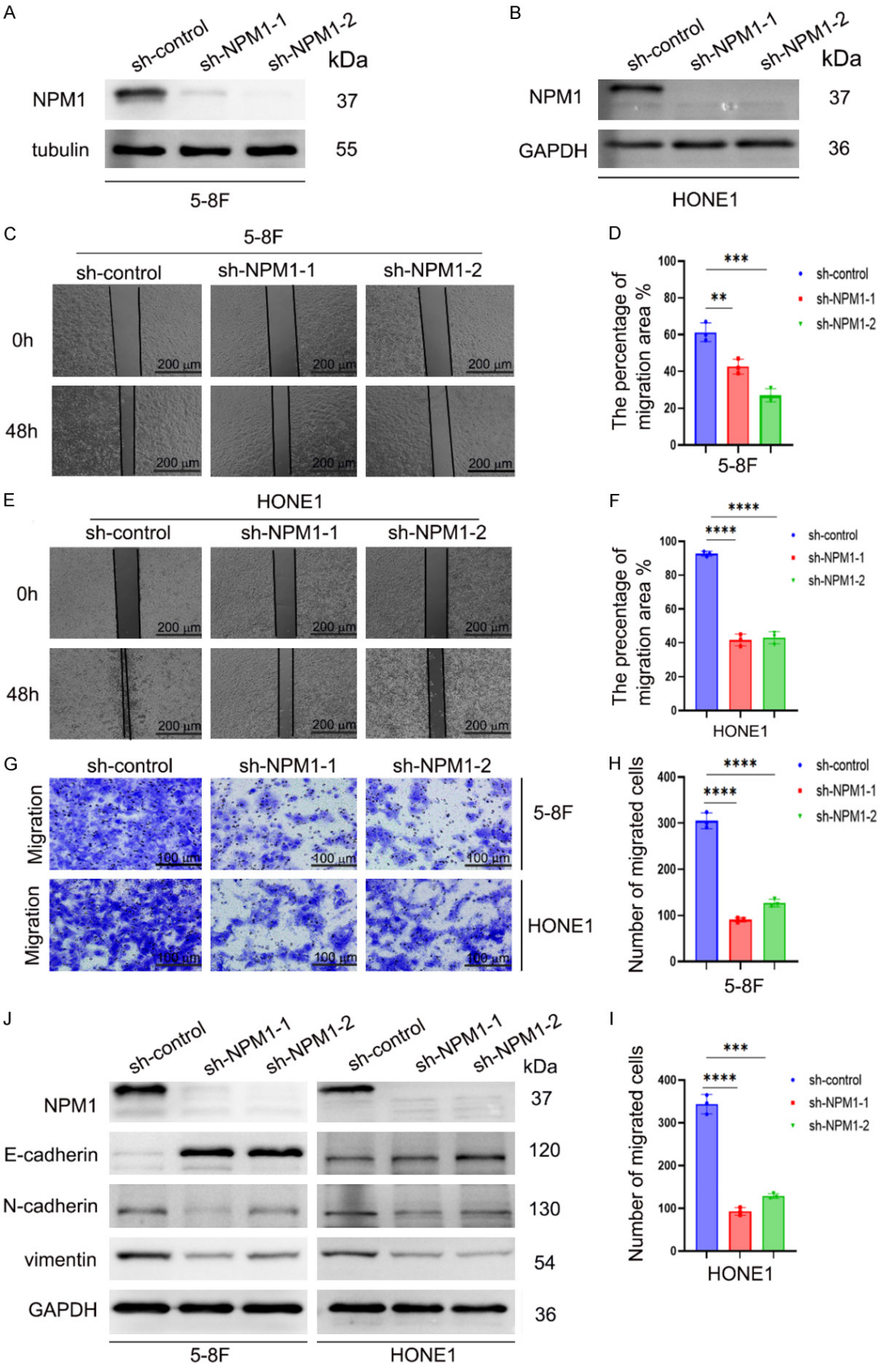
A
sh-control
sh-NPM1-1
sh-NPM1-2
kDa
NPM1
37
tubulin
55
5-8F
B
sh-control
sh-NPM1-1
sh-NPM1-2
kDa
NPM1
37
GAPDH
36
HONE1
C
5-8F
sh-control
sh-NPM1-1
sh-NPM1-2
0h
48h
200 μm
D
The percentage of migration area %
***
**
sh-control
sh-NPM1-1
sh-NPM1-2
5-8F
E
HONE1
sh-control
sh-NPM1-1
sh-NPM1-2
0h
48h
200 μm
F
The precentage of migration area %
****
****
sh-control
sh-NPM1-1
sh-NPM1-2
HONE1
G
sh-control
sh-NPM1-1
sh-NPM1-2
Migration
Migration
100 μm
5-8F
HONE1
H
Number of migrated cells
****
****
sh-control
sh-NPM1-1
sh-NPM1-2
5-8F
J
sh-control
sh-NPM1-1
sh-NPM1-2
sh-control
sh-NPM1-1
sh-NPM1-2
kDa
NPM1
37
E-cadherin
120
N-cadherin
130
vimentin
54
GAPDH
36
5-8F
HONE1
I
Number of migrated cells
***
****
sh-control
sh-NPM1-1
sh-NPM1-2
HONE1

Figure 2. NPM1-knockdown inhibited the migration of NPC cells. A, B. Western blot analysis of the expression of NPM1 in NPC cells infected with lentivirus. C-F. The effect of NPM1 knockdown on the migration of NPC cells at 0 h to 48 h. Bar = 200 μm. Data were presented as the mean ± SD from three independent experiments. $^{**}P < 0.01$; $^{***}P < 0.001$; $^{****}P < 0.0001$, as determined by one-way ANOVA. G-I. The migration ability of 5-8F and HONE1 cells was reduced by NPM1 knockdown. Bar = 100 μm. Data were presented as the mean ± SD from three independent experiments. $^{***}P < 0.001$; $^{****}P < 0.0001$, as determined by one-way ANOVA. J. The expression levels of E-cadherin, N-cadherin, and vimentin in 5-8F and HONE1 cells, as detected by Western blot analysis.

staining revealed that the NPM1-knockdown group exhibited lower expression level of CD44, CD133, and OCT4 compared to the control group (**Figure 5F**; Supplementary Figure 1F). Therefore, these data indicate that NPM1-knockdown inhibited tumor stemness in the NPC cells.

NPM1 found to bind and interact with p53

To understand the functional mechanism of NPM1 in NPC, we used Co-IP and mass spectrometry to identify NPM1-interacting proteins in 5-8F cells. We discovered p53 as a putative interacting protein, by analyzing the predicted interacting proteins determined by mass spectrometry and publicly available protein databases (Supplementary Figure 1C). It is well established that p53 plays a crucial role in preventing the growth of tumors. Cell cycle arrest, apoptosis, and cellular senescence are only a few of the mechanisms by which p53 mediates its anti-tumor role [27]. We also investigated whether NPM1 interacts with p53, and the results of the endogenous co-immunoprecipitation assay (Co-IP) reveal that it does (**Figure 6A**, **6B**). Additionally, according to the immunofluorescence results, NPM1 and p53 were found to be mostly colocalized in the cytoplasm (**Figure 6F**, **6I**). Co-IP examinations of 5-8F and HONE1 cells confirmed that NPM1 interacted with p53 in these cells, as did NPM1 interact with Mdm2 (**Figure 6C**, **6D**), and all were mainly colocalized in the cytoplasm (**Figure 6H**, **6J**). The functional connection between NPM1 and p53 was also investigated by RT-qPCR and western blot analysis. We discovered that the p53 mRNA level was not affected by either NPM1 overexpression or knockdown (Supplementary Figure 1G, 1H). However, it's important to note that NPM1 knockdown elevated p53 protein levels, whereas NPM1 overexpression reduced p53 protein levels (**Figure 6E**, **6G**, **6K**, **6L**). As a result, we assume that post-transcriptional translation is the level at which most of NPM1's influence on p53 occurs.

NPM1 recruited Mdm2 to facilitate the proteasomal degradation of p53 by inducing ubiquitination

The E3 ubiquitin ligase Mdm2 is an important inhibitor of p53 which can suppress p53 protein level via constitutive proteasomal degradation in normal, unstressed cells [26]. Since our data above indicated that NPM1 decreased the protein level of p53 and that NPM1 interacted with Mdm2, we speculated that NPM1 might promote nasopharyngeal carcinoma metastasis and stemness by recruiting Mdm2 to induce the ubiquitin-mediated degradation of p53 in NPC. Thus, a cycloheximide (CHX) chase experiment was performed to determine whether the overexpression of NPM1 affected the half-life of p53 in order to substantiate this argument. The findings show that the half-life of p53 was considerably shorter in the NPM1-overexpressing cells than in the control cells (**Figure 7A-D**). Importantly, this NPM1-induced downregulation of p53 could be reversed by the treatment of proteasome inhibitor MG132 (**Figure 7E**, **7F**). Then, depending on Mdm2 expression, the immunoprecipitation and western blotting results show that the overexpression of NPM1 enhanced p53 ubiquitination (**Figure 7G**, **7H**). These findings reveal that Mdm2 was recruited by NPM1 to facilitate the ubiquitin-mediated proteasomal degradation of p53.

p53 reversed the migration and tumor stemness induced by NPM1 in NPC

Given the data above that NPM1 suppressed p53 protein level, we hypothesized that NPM1 might serve as a cellular oncogene. Rescue experiments were then conducted to test this hypothesis. We transfected the siRNA of p53 into NPM1-knockdown stable cells, and performed wound healing assay. The results showed that NPM1 knockdown attenuated the migration of 5-8F and HONE1 cells, which could be reversed by p53 knockdown (**Figure 8D**). When p53 siRNA was transfected into 5-8F and

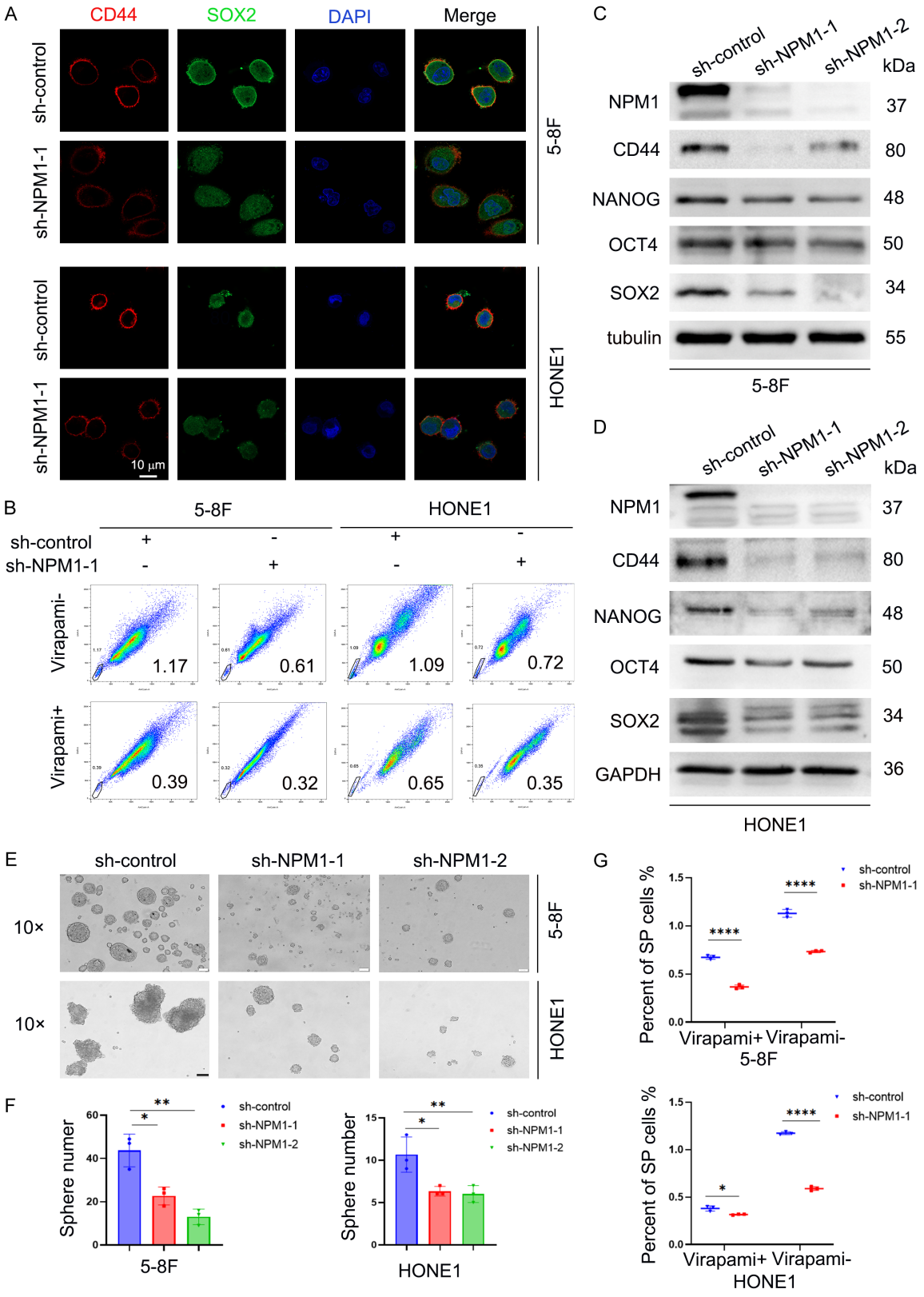

Figure 3. NPM1 knockdown inhibited tumor stemness properties in NPC cells. A. The relative fluorescence intensity of CD44 and SOX2 was assessed by immunofluorescence staining. Bar = 10 μm. B, G. Side population assay revealed that NPM1 knockdown inhibited NPC stemness. Data were presented as the mean ± SD from two independent experiments. ***P < 0.001; ****P < 0.0001, as determined by the Student's t-test. C, D. The expression levels of

CD44, NANOG, OCT4, and SOX2, as detected by Western blot analysis. E, F. Tumorsphere formation assay revealed that NPM1 knockdown inhibited NPC stemness. Bar = 200 μm. Data were presented as the mean ± SD from three independent experiments. *P < 0.05; **P < 0.01, as determined by one-way ANOVA.

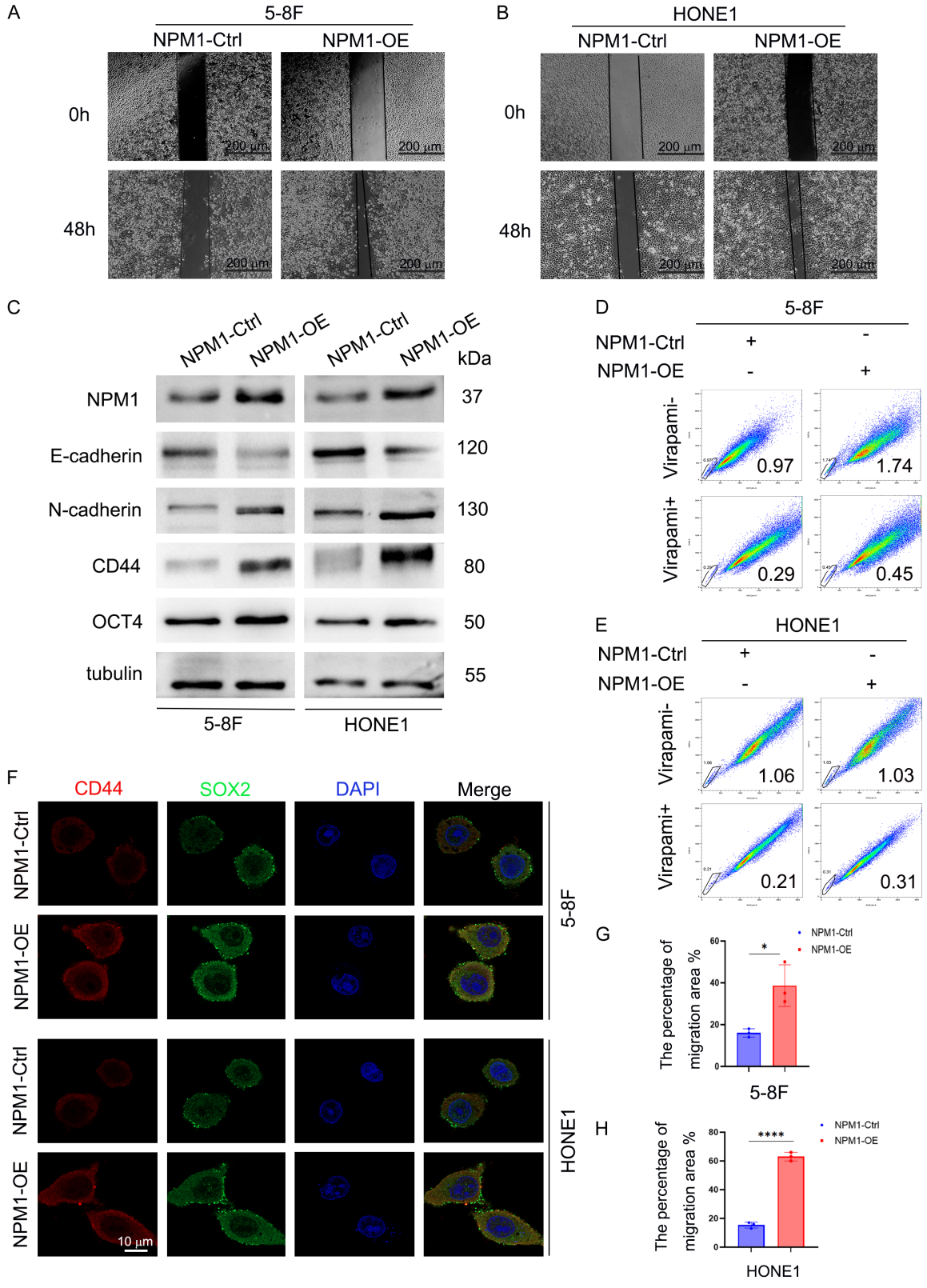

Figure 4. NPM1 overexpression promoted the migration and tumor stemness properties of NPC cells. A, B, G, H. Wound healing assay showed the enhanced migratory ability of 5-8F and HONE1 cells by NPM1 overexpression. Bar = 200 μm. $^{*}P < 0.05$; $^{****}P < 0.0001$, as determined by the Student's t-test. C. The expression levels of E-cadherin, N-cadherin, CD44, and OCT4 in 5-8F and HONE1 cells, as detected by Western blot analysis. D, E. Side population assay indicated that the overexpression of NPM1 promoted NPC stemness. F. The relative fluorescence intensities of CD44 and SOX2, as assessed by immunofluorescence staining. Bar = 10 μm.

Table 3. The side population ratio between control group and sh-NPM1 group

5-8F	sh-control	sh-NPM1-1
Virapami-	1.17	0.61
Virapami+	0.39	0.32
HONE1	sh-control	sh-NPM1-1
Virapami-	1.09	0.72
Virapami+	0.65	0.35

Table 4. The side population ratio between control group and NPM1-overexpression group

5-8F	NPM1-Ctrl	NPM1-OE
Virapami-	0.97	1.74
Virapami+	0.29	0.45
HONE1	NPM1-Ctrl	NPM1-OE
Virapami-	1.06	1.03
Virapami+	0.21	0.31

HONE1 cells, the wound healing assay detected an increased migration rate compared to the control cells (**Figure 8D**). Furthermore, immunofluorescence staining demonstrated that p53 knockdown NPC cells expressed CSC markers (CD44 and SOX2) at greater levels compared to control cells (**Figure 8C**). In contrast, NPC cells with both NPM1- and p53-knockdown displayed similar fluorescence intensities of CD44 and SOX2 to the control group (**Figure 8C**). Moreover, we found that p53 knockdown increased N-cadherin, vimentin, CD44, and SOX2 levels while decreased E-cadherin levels in NPC cells. By transfecting NPM1-knockdown NPC cells with siRNA targeting p53, these phenomena were reversed (**Figure 8A**, **8B**). Taken together, these data suggest that NPM1 regulates the migration and the tumor stemness of NPC cells by inhibiting the activity and function of p53.

Discussion

The non-ribosomal nucleolar phosphoprotein known as nucleophosmin (NPM), B23, numatrin, and NO38, was first identified to be present in large concentrations in the granular portion of the nucleolus [28]. The fact that NPM1 is linked to the development of human tumors has aroused research interest in the gene encoding this protein [6]. While controversy exists regarding the precise role of NPM1 in various malignancies [29-34], systematic methodologies have not yet been applied to explore the biological function of NPM1 in NPC in depth. Meanwhile, the cancer heterogeneity of NPC that uniquely characterizes this form of cancer suggests that the complexity and novelty of its underlying mechanisms require research into the precise role of NPM1. In this study, we used both in vitro and in vivo experiments to explore the function and its underlying mechanism of NPM1 in the progression and metastasis of NPC. Our findings provide insight into the regulatory role of NPM1 in NPC. We revealed that NPM1 promoted the malignancy of NPC partially through the reduction of p53, whereby p53 and its associated signaling pathways were inhibited by NPM1. Typical CSC characteristics and the migration ability of NPC cells were both promoted by this reduction in p53. In particular, NPC progression was prevented by NPM1 inhibition, suggesting that NPM1 may be used as an alternative therapeutic target for the treatment of NPC.

First, we discovered that NPM1 expression was upregulated in NPC tissues, as determined by bioinformatics analysis using data from the GEO database. In addition, immunohistochemical analysis confirmed that NPM1 expression was higher in NPC tissues than in noncancerous nasopharyngeal tissues. Furthermore, tissue microarray data showed that the expression level of NPM1 was correlated with distant metastases and the clinical stage, suggesting that NPM1 might be involved in the development and metastasis of NPC. Consistently, we found that patients with high levels of NPM1 had worse overall survival. These findings provide evidence for the clinical application of

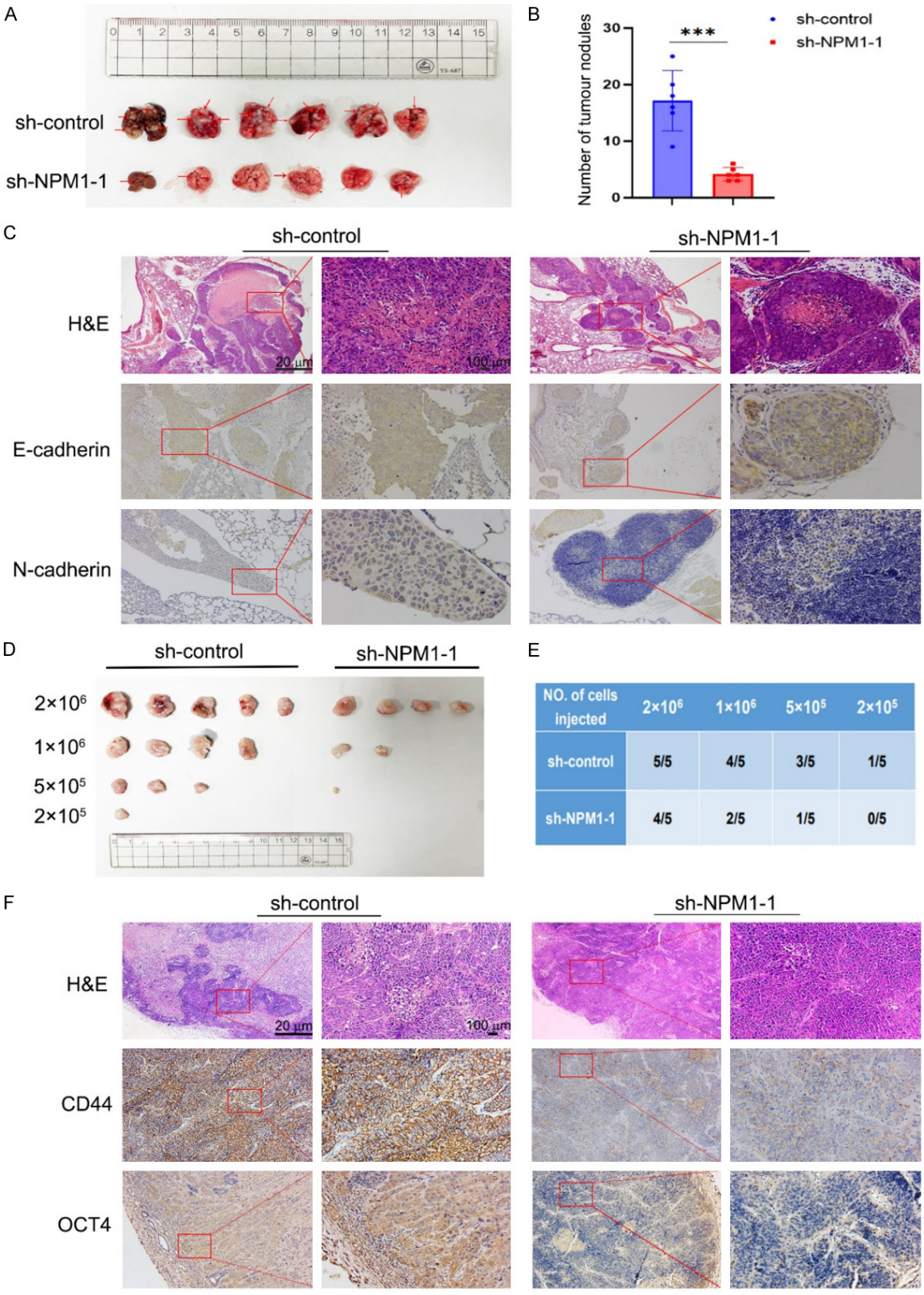

NO. of cells injected	2×10^6	1×10^6	5×10^5	2×10^5
sh-control	5/5	4/5	3/5	1/5
sh-NPM1-1	4/5	2/5	1/5	0/5

Figure 5. NPM1 promoted the metastasis of NPC and tumor stemness in mouse model. A. Lungs were collected 6 weeks after tail injection of NPC cells (n = 6). B. The number of tumor nodules in the lungs. ***P < 0.001, as determined by the Student's t-test. C. Representative H&E and IHC staining results of the harvested lung samples from control and NPM1 knockdown mice. Bar = 100 μm. D, E. Tumor formation in nude mice injected with 2×10^6, 1×10^6, 5×10^5 or 2×10^5 NPM1-knockdown or control cells (n = 5). F. Representative H&E and IHC staining results of the dissected tumor tissues. Bar = 100 μm.

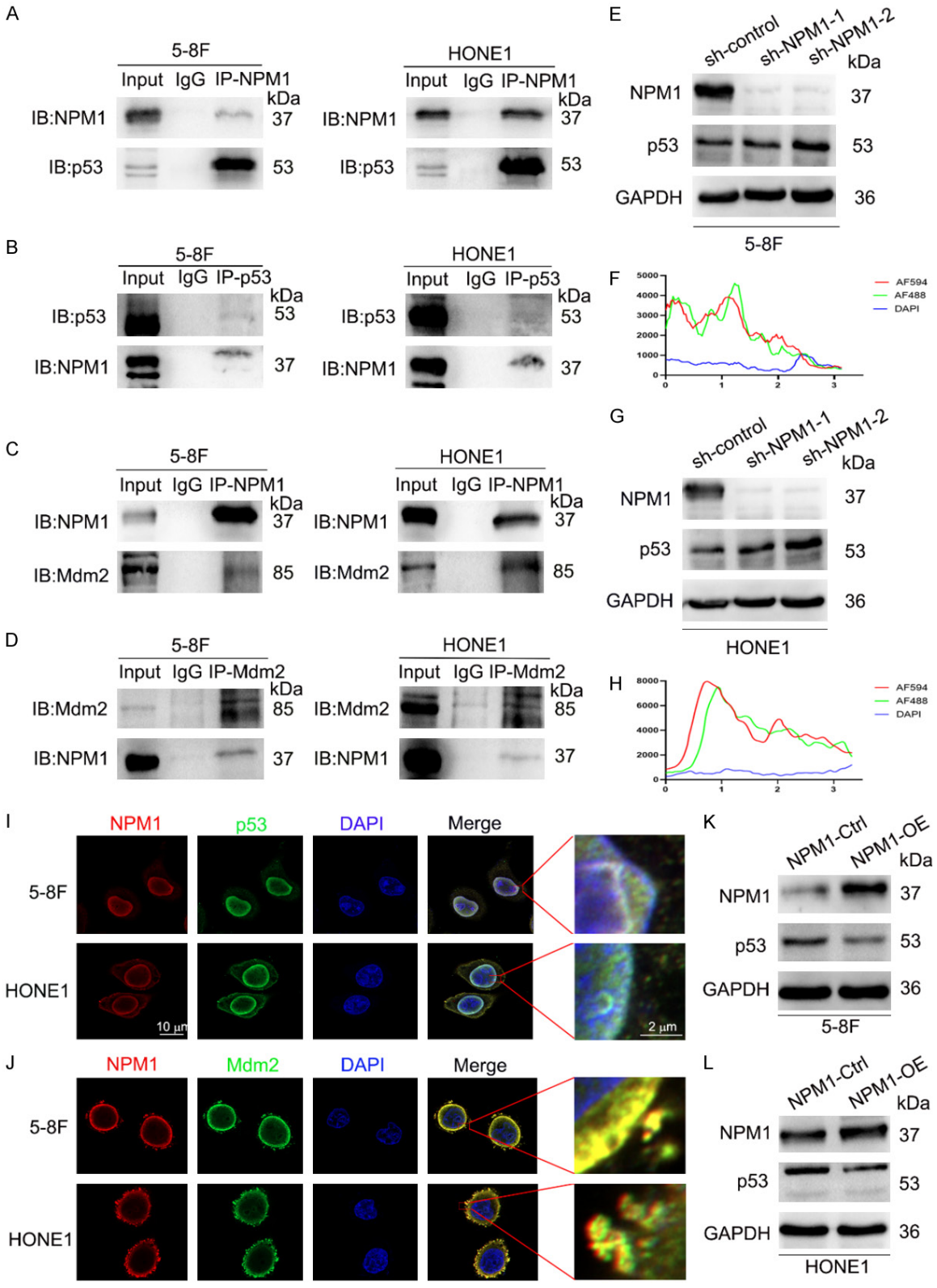

Figure 6. NPM1 interacted with p53 and Mdm2. A, B. Co-IP coupled Western blot analysis indicated the interaction between NPM1 and p53. C, D. Co-IP coupled Western blot analysis indicated the interaction between NPM1 and Mdm2. I, F. Representative images of the immunofluorescent staining of NPM1 (red) and p53 (green). Bar = 10 μm. J, H. Representative images of the immunofluorescent staining of NPM1 (red) and Mdm2 (green). Bar = 10 μm. E, G, K, L. The protein level of p53 in either NPM1 overexpression or NPM1 knockdown cells was detected by Western blot analysis.

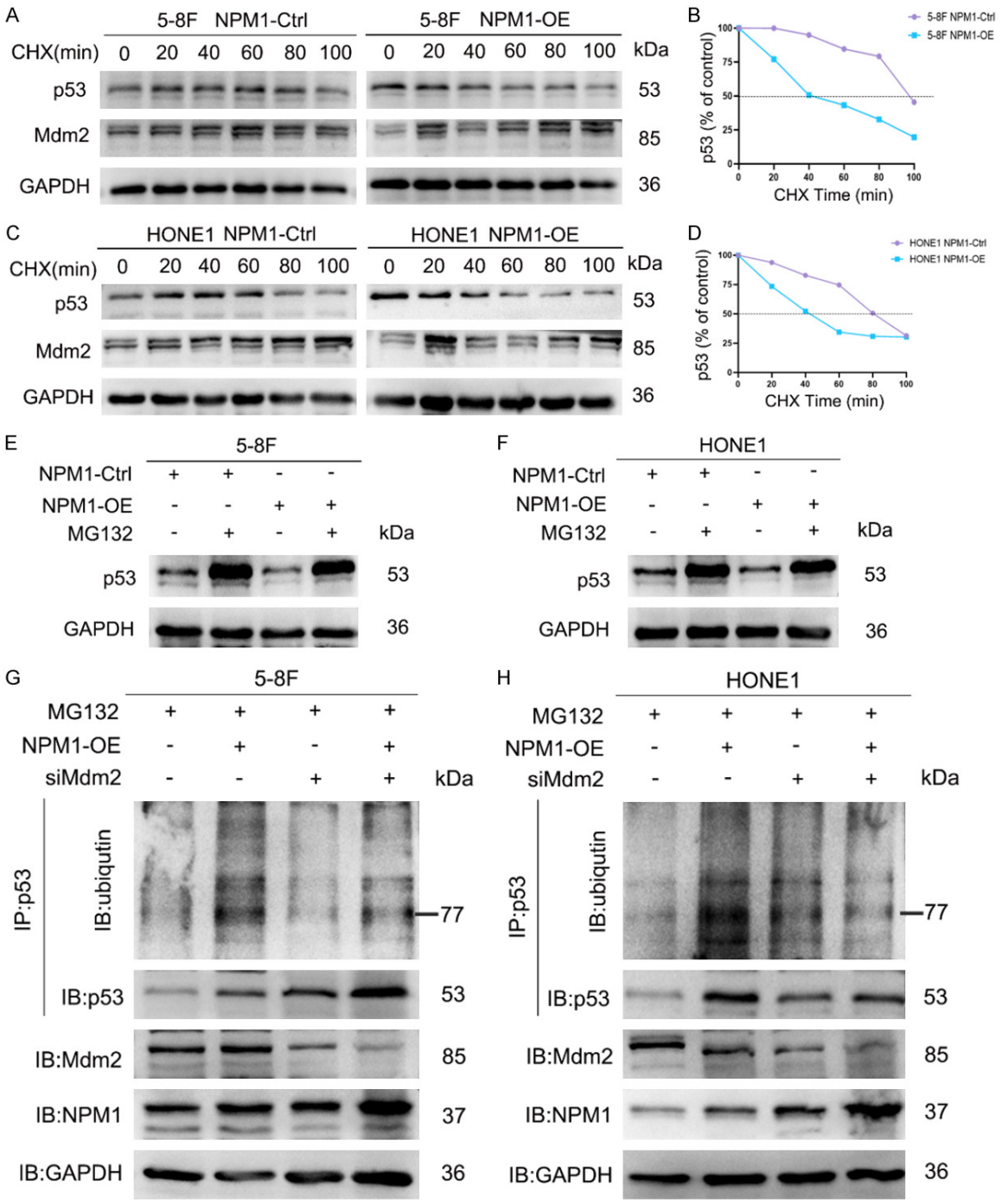

Figure 7. NPM1 induced the ubiquitin-mediated proteasome degradation of p53 by recruiting Mdm2. A, C. Cycloheximide (CHX) chase analysis of the half-life of p53 in control and NPM1-overexpressing 5-8F and HONE1 cells. CHX: 50 μg/ml. B, D. The half-life of p53 in 5-8F and HONE1 cells. E, F. The effects of DMSO or MG132 (20 μM) on the stability of p53 protein in the control and NPM1-overexpressing cells. G, H. The effect of NPM1 overexpression and siMdm2 on the ubiquitination of p53 was determined by Co-IP and Western blot analysis.

NPM1 as a predictive marker for the prognosis of patients with NPC.

Intriguingly, we discovered that the overexpression of NPM1 enhanced both the tumor stem-

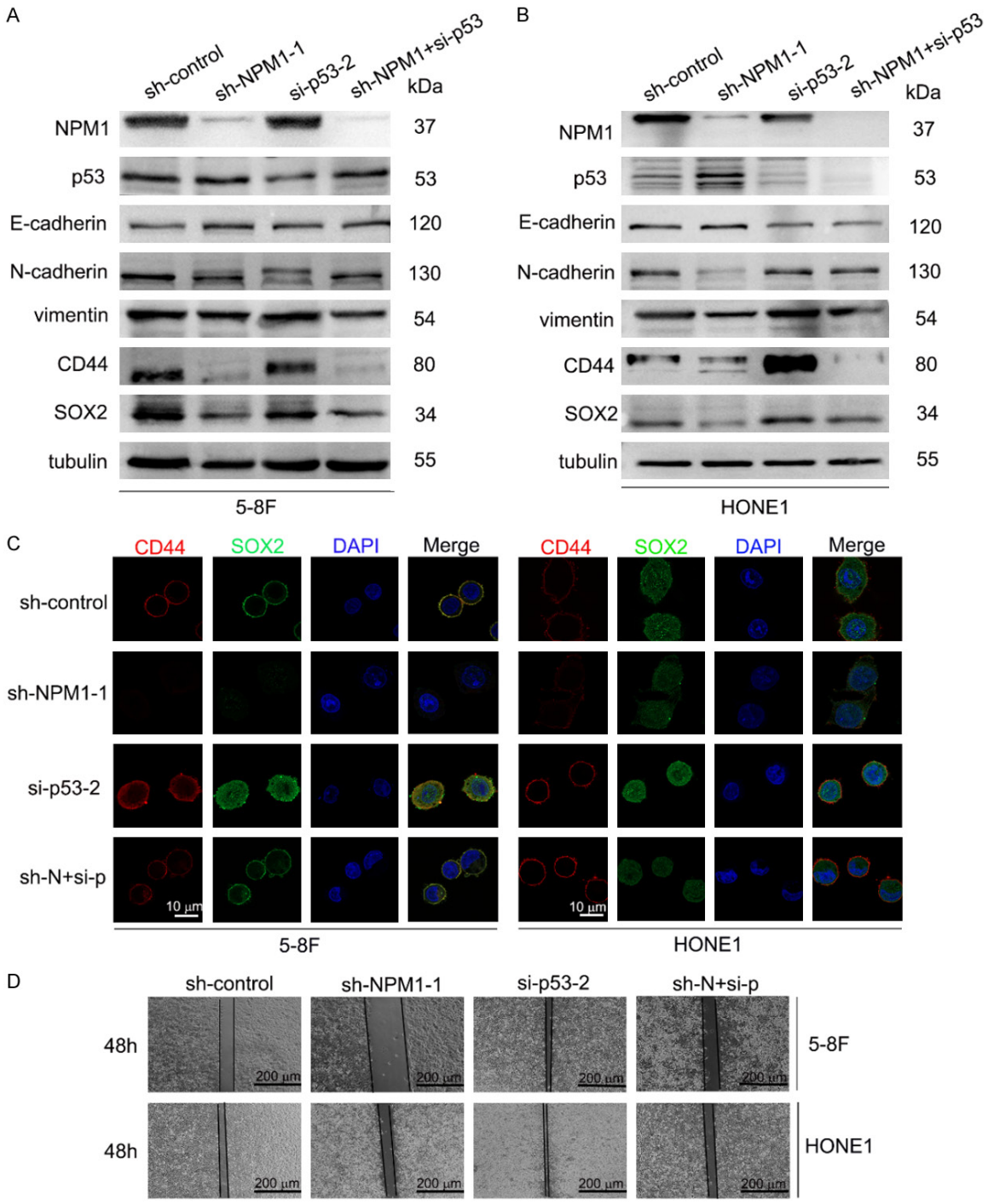

Figure 8. p53 reversed cell migration and tumor stemness induced by NPM1 in NPC. A, B. The protein levels of NPM1, p53, E-cadherin, N-cadherin, vimentin, CD44, SOX2, and tubulin in the sh-control group, sh-NPM1-1 group, si-p53-2 group, and sh-NPM1+si-p53 group were detected by Western blot analysis. C. Immunofluorescence staining of CD44 and SOX2 in the sh-control group, sh-NPM1-1 group, si-p53-2 group, and sh-NPM1+si-p53 group. Bar = 10 μm. D. Cell migration in the sh-control group, sh-NPM1-1 group, si-p53-2 group, and sh-NPM1+si-p53 group was determined by wound healing assay. Bar = 200 μm.

ness and the migration of NPC cells, whereas NPM1 knockdown dramatically decreased these two properties. Our mouse xenograft model and lung metastasis model further demonstrated the oncogenic role of NPM1 by promoting both tumor stemness and metastasis.

These two properties are further described below.

EMT is a molecular process involved in conferring the ability of metastasis in cancer cells [35]. Cells acquire mesenchymal cell phenotypes as a result of losing cell-cell and cell-extracellular matrix adhesion during EMT. This enables the separation of distant organs and surrounding tissues as well as the detachment of cells from the original tumor. Embryonic morphogenesis, tissue fibrosis, wound healing and cancer cell metastasis are all significantly influenced by the EMT process [36]. Regarding the property of tumor stemness, accumulating evidence indicates that the metastasis of cancer cells initiates from the population of CSCs [37]. Interestingly, in this study, we discovered that NPM1 directly induced EMT by suppressing E-cadherin expression while enhancing the expression of N-cadherin and vimentin. Meanwhile, NPM1 increased the protein levels of CSC-specific markers, including CD44, OCT4, and SOX2. Together, our study revealed a novel functional of NPM1 in promoting NPC metastasis, which has not yet previously been established.

Furthermore, we set about investigating the molecular mechanism underlying the function of NPM1 in the above processes. By using Co-IP in conjunction with mass spectrometry in NPM1-overexpressing 5-8F cells, we identified p53 as a potential NPM1-interacting protein. p53 is a well-studied tumor suppressor with a very short half-life; therefore, it is maintained at a low, often undetectable level in normal cells [38]. Emerging evidence indicates that wild-type p53 possesses greater tumor-suppressive capability compared to mutant p53, which is often oncogenic [39]. Herein, we discovered that NPM1 modulated p53 protein level without affecting its mRNA level. Notably, both MG132 treatment and CHX chase assay revealed that the overexpression of NPM1 reduced the stability of p53 and shorten its half-life. In support with these data, in vitro ubiquitination experiments also demonstrated that NPM1 overexpression significantly increased the ubiquitination of p53. Therefore, we concluded that NPM1 controls the p53 protein level through regulating the ubiquitination-proteasome degradation of p53. NPM1, however, lacks the capacity to transfer ubiquitin. Moreover, we discovered NPM1 interacted with Mdm2, an inhibitor of p53's tumor-suppressive activities, may be recruited by NPM1 [40]. Mdm2 binds to the transcriptional activation domain of p53 and prevents it from modulating target genes to exert an antiproliferative impact [41]. Now, we can confirm that Mdm2 also promotes p53's degradation in circumstances where p53 is otherwise stable, thereby regulating the downstream NPM1-related tumor stemness properties and EMT signals.

In conclusion, our study initially revealed the oncogenic role of NPM1 in NPC. Mechanistically, NPM1 physically interacted with p53 to prevent it from nuclear translocation, thereby promoting NPC cell metastasis and stemness. This study provides the following insight; the elucidation of a novel mechanism by which NPM1 recruits Mdm2 to promote the ubiquitin-mediated degradation of p53, which results in the inhibition of the p53-related signaling pathway both in vitro and in vivo. NPM1 may therefore be a promising indicator for NPC and its prognosis, as well as a potential therapeutic target.

Acknowledgements

This work was supported by National Natural Science Foundation of China (grant number: 81572666); Guangzhou Science and Technology Project (grant number: 201707010382, 202102080071).

Disclosure of conflict of interest

None.

Address correspondence to: Dr. Hong Peng, Department of Otolaryngology-Head and Neck Surgery, Guangdong Second Provincial General Hospital, The Compound at No. 466 Middle Xingang Road, Haizhu District, Guangzhou 510220, Guangdong, China. E-mail: doctorpenghong@163.com

References

[1] Chen YP, Chan ATC, Le QT, Blanchard P, Sun Y and Ma J. Nasopharyngeal carcinoma. Lancet 2019; 394: 64-80.

[2] Ren X, Yang X, Cheng B, Chen X, Zhang T, He Q, Li B, Li Y, Tang X, Wen X, Zhong Q, Kang T, Zeng M, Liu N and Ma J. HOPX hypermethylation promotes metastasis via activating SNAIL transcription in nasopharyngeal carcinoma. Nat Commun 2017; 8: 14053.

[3] Zhen Y, Fang W, Zhao M, Luo R, Liu Y, Fu Q, Chen Y, Cheng C, Zhang Y and Liu Z. miR-374a-CCND1-pPI3K/AKT-c-JUN feedback loop modulated by PDCD4 suppresses cell growth, metastasis, and sensitizes nasopharyngeal carcinoma to cisplatin. Oncogene 2017; 36: 275-285.
[4] Chan AT, Grégoire V, Lefebvre JL, Licitra L and Felip E. Nasopharyngeal cancer: EHNS-ESMO-ESTRO clinical practice guidelines for diagnosis, treatment and follow-up. Ann Oncol 2010; 21 Suppl 5: v187-189.
[5] Wu L, Li C and Pan L. Nasopharyngeal carcinoma: a review of current updates. Exp Ther Med 2018; 15: 3687-3692.
[6] Grisendi S, Mecucci C, Falini B and Pandolfi PP. Nucleophosmin and cancer. Nat Rev Cancer 2006; 6: 493-505.
[7] Chang JH and Olson MO. Structure of the gene for rat nucleolar protein B23. J Biol Chem 1990; 265: 18227-18233.
[8] Wang D, Umekawa H and Olson MO. Expression and subcellular locations of two forms of nucleolar protein B23 in rat tissues and cells. Cell Mol Biol Res 1993; 39: 33-42.
[9] Hingorani K, Szebeni A and Olson MO. Mapping the functional domains of nucleolar protein B23. J Biol Chem 2000; 275: 24451-24457.
[10] Tanaka M, Sasaki H, Kino I, Sugimura T and Terada M. Genes preferentially expressed in embryo stomach are predominantly expressed in gastric cancer. Cancer Res 1992; 52: 3372-3377.
[11] Nozawa Y, Van Belzen N, Van der Made AC, Dinjens WN and Bosman FT. Expression of nucleophosmin/B23 in normal and neoplastic colorectal mucosa. J Pathol 1996; 178: 48-52.
[12] Shields LB, Gerçel-Taylor C, Yashar CM, Wan TC, Katsanis WA, Spinnato JA and Taylor DD. Induction of immune responses to ovarian tumor antigens by multiparity. J Soc Gynecol Investig 1997; 4: 298-304.
[13] Subong EN, Shue MJ, Epstein JI, Briggman JV, Chan PK and Partin AW. Monoclonal antibody to prostate cancer nuclear matrix protein (PRO:4-216) recognizes nucleophosmin/B23. Prostate 1999; 39: 298-304.
[14] Tsui KH, Cheng AJ, Chang Pe, Pan TL and Yung BY. Association of nucleophosmin/B23 mRNA expression with clinical outcome in patients with bladder carcinoma. Urology 2004; 64: 839-844.
[15] Nieto MA, Huang RY, Jackson RA and Thiery JP. EMT: 2016. Cell 2016; 166: 21-45.
[16] Mittal V. Epithelial mesenchymal transition in tumor metastasis. Annu Rev Pathol 2018; 13: 395-412.
[17] Gupta PB, Fillmore CM, Jiang G, Shapira SD, Tao K, Kuperwasser C and Lander ES. Stochastic state transitions give rise to phenotypic equilibrium in populations of cancer cells. Cell 2011; 146: 633-644.
[18] Kreso A and Dick JE. Evolution of the cancer stem cell model. Cell Stem Cell 2014; 14: 275-291.
[19] Zhang P, Liu Y, Lian C, Cao X, Wang Y, Li X, Cong M, Tian P, Zhang X, Wei G, Liu T and Hu G. SH3RF3 promotes breast cancer stem-like properties via JNK activation and PTX3 upregulation. Nat Commun 2020; 11: 2487.
[20] Li J, Zhang X, Sejas DP and Pang Q. Negative regulation of p53 by nucleophosmin antagonizes stress-induced apoptosis in human normal and malignant hematopoietic cells. Leuk Res 2005; 29: 1415-1423.
[21] Appella E and Anderson CW. Post-translational modifications and activation of p53 by genotoxic stresses. Eur J Biochem 2001; 268: 2764-2772.
[22] Ashcroft M, Kubbutat MH and Vousden KH. Regulation of p53 function and stability by phosphorylation. Mol Cell Biol 1999; 19: 1751-1758.
[23] Brooks CL and Gu W. Ubiquitination, phosphorylation and acetylation: the molecular basis for p53 regulation. Curr Opin Cell Biol 2003; 15: 164-171.
[24] Boyd SD, Tsai KY and Jacks T. An intact HDM2 RING-finger domain is required for nuclear exclusion of p53. Nat Cell Biol 2000; 2: 563-568.
[25] Freedman DA and Levine AJ. Nuclear export is required for degradation of endogenous p53 by MDM2 and human papillomavirus E6. Mol Cell Biol 1998; 18: 7288-7293.
[26] Hassin O and Oren M. Drugging p53 in cancer: one protein, many targets. Nat Rev Drug Discov 2023; 22: 127-144.
[27] Vogelstein B, Lane D and Levine AJ. Surfing the p53 network. Nature 2000; 408: 307-310.
[28] Lim MJ and Wang XW. Nucleophosmin and human cancer. Cancer Detect Prev 2006; 30: 481-490.
[29] You BJ, Huang IJ, Liu WH, Hung YB, Chang JH and Yung BY. Decrease in nucleophosmin/B23 mRNA and telomerase activity during indomethacin-induced apoptosis of gastric KATO-III cancer cells. Naunyn Schmiedebergs Arch Pharmacol 1999; 360: 683-690.
[30] Skaar TC, Prasad SC, Sharareh S, Lippman ME, Brünner N and Clarke R. Two-dimensional gel electrophoresis analyses identify nucleophosmin as an estrogen regulated protein associated with acquired estrogen-independence in human breast cancer cells. J Steroid Biochem Mol Biol 1998; 67: 391-402.
[31] Redner RL, Rush EA, Faas S, Rudert WA and Corey SJ. The t(5;17) variant of acute promy-

elocytic leukemia expresses a nucleophosmin-retinoic acid receptor fusion. Blood 1996; 87: 882-886.
[32] Morris SW, Kirstein MN, Valentine MB, Dittmer KG, Shapiro DN, Saltman DL and Look AT. Fusion of a kinase gene, ALK, to a nucleolar protein gene, NPM, in non-Hodgkin's lymphoma. Science 1994; 263: 1281-1284.
[33] Mendes-da-Silva P, Moreira A, Duro-da-Costa J, Matias D and Monteiro C. Frequent loss of heterozygosity on chromosome 5 in non-small cell lung carcinoma. Mol Pathol 2000; 53: 184-187.
[34] Léotoing L, Meunier L, Manin M, Mauduit C, Decaussin M, Verrijdt G, Claessens F, Benahmed M, Veyssière G, Morel L and Beaudoin C. Influence of nucleophosmin/B23 on DNA binding and transcriptional activity of the androgen receptor in prostate cancer cell. Oncogene 2008; 27: 2858-2867.
[35] Babaei G, Aziz SG and Jaghi NZZ. EMT, cancer stem cells and autophagy; the three main axes of metastasis. Biomed Pharmacother 2021; 133: 110909.
[36] Lo UG, Lee CF, Lee MS and Hsieh JT. The role and mechanism of epithelial-to-mesenchymal transition in prostate cancer progression. Int J Mol Sci 2017; 18: 2079.
[37] Tang KD, Holzapfel BM, Liu J, Lee TK, Ma S, Jovanovic L, An J, Russell PJ, Clements JA, Hutmacher DW and Ling MT. Tie-2 regulates the stemness and metastatic properties of prostate cancer cells. Oncotarget 2016; 7: 2572-2584.
[38] Kubbutat MH, Jones SN and Vousden KH. Regulation of p53 stability by Mdm2. Nature 1997; 387: 299-303.
[39] Amit M, Takahashi H, Dragomir MP, Lindemann A, Gleber-Netto FO, Pickering CR, Anfossi S, Osman AA, Cai Y, Wang R, Knutsen E, Shimizu M, Ivan C, Rao X, Wang J, Silverman DA, Tam S, Zhao M, Caulin C, Zinger A, Tasciotti E, Dougherty PM, El-Naggar A, Calin GA and Myers JN. Loss of p53 drives neuron reprogramming in head and neck cancer. Nature 2020; 578: 449-454.
[40] Haupt Y, Barak Y and Oren M. Cell type-specific inhibition of p53-mediated apoptosis by mdm2. EMBO J 1996; 15: 1596-1606.
[41] Berberich S and Cole M. The mdm-2 oncogene is translocated and overexpressed in a murine plasmacytoma cell line expressing wild-type p53. Oncogene 1994; 9: 1469-1472.

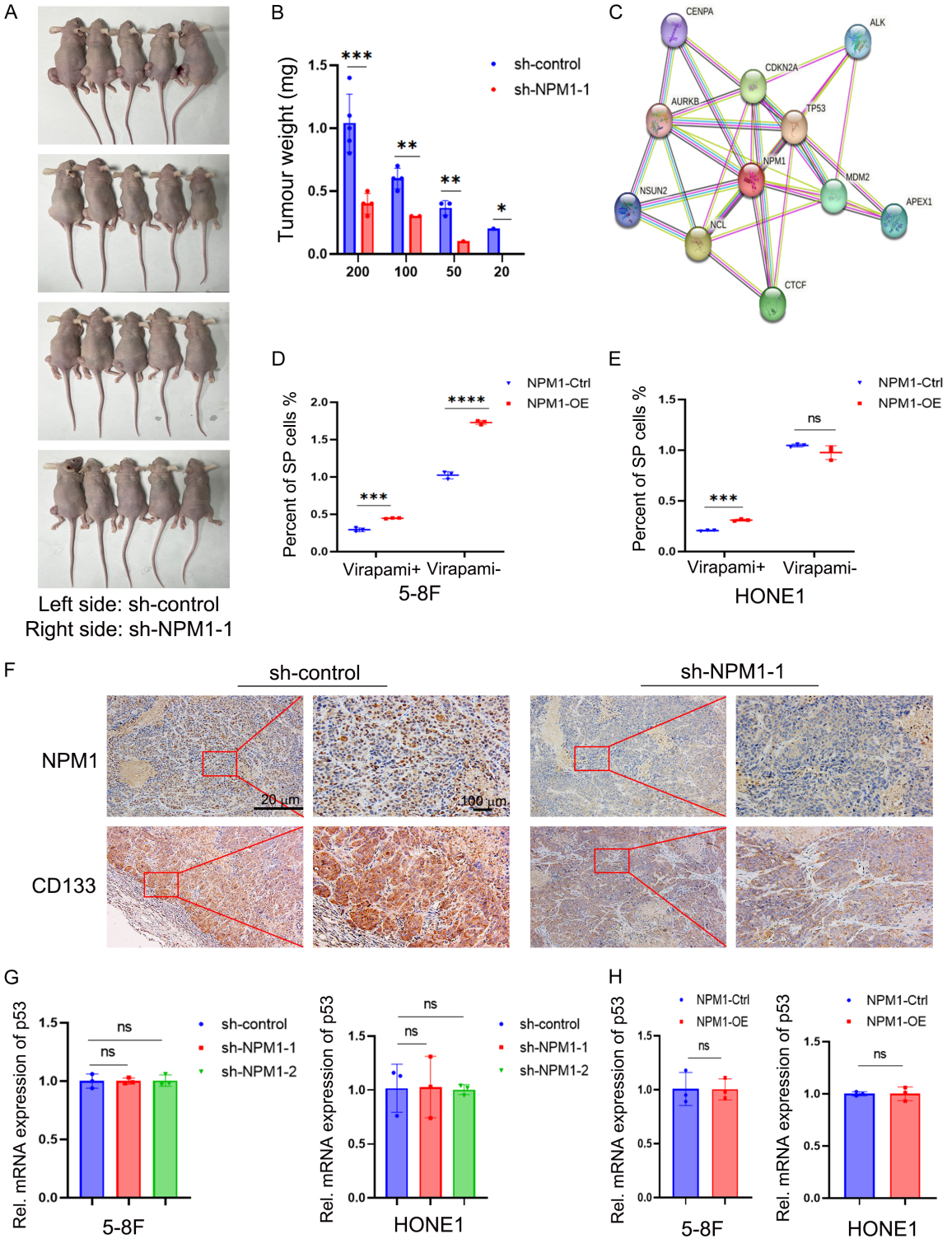

Supplementary Figure 1. A, B. Nude mice were subcutaneously transplanted with control or NPM1-knockdown 5-8F cells, and the tumor weights were measured. C. Mutual effects between NPM1 and other proteins were shown using a protein association networks data set of STRING. D, E. Side population assay indicated that NPM1 overexpression promoted NPC stemness. Data were presented as the mean ± SD from two independent experiments. ***P < 0.001; ****P < 0.0001, as determined by the Student's t-test. F. Representative IHC staining results of the dissected tumor tissues. Bar = 100 μm. G. The mRNA level of p53 was examined in NPM1 knockdown cells by RT-qPCR. H. The mRNA level of p53 was assessed in NPM1 overexpressing cells by RT-qPCR.